DTC Enabled Frequency Tunable Inverted-F Antenna for IoT Applications

Thomas Houret, Leonardo Lizzi, *Member, IEEE,* Fabien Ferrero, *Member, IEEE,* Christophe Danchesi, and Stephane Boudaud

***Abstract*—In this paper, an integrated frequency tunable Inverted-F Antenna (IFA) is presented. Thanks to a reconfigurable circuit using a Digitally Tunable Capacitor (DTC), the antenna resonant frequency can be shifted over 32 different positions from 600 to 960 MHz. This tunability is used to compensate the frequency detuning caused by the change in the antenna close surrounding. The small dimensions as well as the digital control and the low power consumption of the reconfiguration circuit make the proposed antenna a good candidate for IoT applications.**

***Index Terms*—Frequency tunable antenna, reconfigurable antenna, integrated antenna, internet-of-things (IoT), digitally tunable capacitor (DTC), inverted-F antenna (IFA).**

I. Introduction

INTERNET of things (IoT) systems usually do not require wide frequency bandwidths since the amount of information to be transmitted is very limited. Antennas for IoT devices can therefore have a high Q-factor [2], thus allowing for miniaturization of the radiating system [3]. However, narrowband antennas naturally suffer from high sensitivity to the environment. Moreover, IoT terminal are usually deeply integrated in various objects with different materials. A small variation of the characteristics of the surroundings of the antenna causes a shift of the antenna resonant frequency, resulting in an impedance mismatching at the operating frequency.

A possible solution for compensating the effects of the environment is to use frequency-agile antennas (a recent overview can be found in [4]). The idea is to integrate into the antenna one or more active reconfigurable components, which can be electronically controlled to re-tune the antenna resonant frequency in the transceiver operating band, whatever the antenna surroundings.

An antenna structure suitable for IoT devices, which has been popularly adopted for mobile handsets, is the Inverted-F Antenna (IFA) or, similarly, the Planar IFA (PIFA). The low profile makes the IFA suitable for integration, while its low cost and easy fabrication allow for mass production, as required for IoT devices. A frequency reconfigurable PIFA is presented in [5]. The operation frequency is tuned by varactor diodes integrated in the antenna geometry. A varactor is also used in [6] to reconfigure the frequency of a 3D IFA for digital video broadcasting applications. Varactors however cannot be used for IoT applications since their control require high voltages (up to 23 V in [5]) usually not available on battery powered IoT devices, and because of their low power handling, which limits their use only in the receiving mode. Differently, in [7] the PIFA frequency is reconfigured through PIN diodes that are used to change the position of the PIFA shorting pin. Such a solution however requires the use of 4 reconfigurable components to enable only 4 different antenna states. This hardly meets the limited control chains available on a IoT device. A better ratio between the number of states and used components is obtained in [8], where, thanks to a geometry based on nested slots, a reconfigurable PIFA enables 4 different states using only 2 PIN diodes. Nevertheless, the simple ON-OFF capability of PIN diodes makes the use of these components more suitable to provide multiband operation rather then enabling the fine tuning of the antenna resonance. Recently, Digitally Tunable Capacitors (DTC) and MEMS varactors have been proposed for tunable RF systems with a high power handling (>30 dBm) and a digital control. Eventhough the DTC has a lower quality factor than a MEMS component [9], [10], this technology is more mature for an industrial project.

In this paper, a frequency tunable IFA suitable for integration in a compact and battery powered IoT device is presented. The frequency reconfiguration capability is used to counterbalance the shift of the antenna resonant frequency produced by the variation of the close environment surrounding the IoT device. This allows the maximization of the antenna total efficiency whatever the operation condition. The reconfiguration mechanism relies on the use of a single DTC component, which provides 32 different capacitance states. This enables a fine tuning of the antenna resonant frequency without increasing the complexity of the control circuit.

II. Antenna Structure

The structure of the proposed frequency tunable antenna as integrated into the miniature IoT tracking device is shown in Fig. 1. The antenna, which is based on the IFA concept [11], is constituted by a metallic arm (shown in red) mounted above the ground plane that is printed on the back of a printed circuit board (PCB) of dimensions $L_1 \times W_2$ (in green). The PCB is made of a standard FR4 dielectric substrate of thickness 1.6 mm ($\epsilon_r = 4.3, \tan\delta = 0.025$). The antenna is shorted to the ground by a vertical metallic strip located at a distance f_p from the feeding point. The final part of the antenna arm is

T. Houret, L. Lizzi and F. Ferrero are with the Université Côte d'Azur, CNRS, LEAT, Sophia Antipolis, France. e-mail: leonardo.lizzi@univ-cotedazur.fr.

C. Danchesi and S. Boudaud are with Abeeway, Sophia Antipolis, France. e-mail: stephane.boudaud@abeeway.com.

Manuscript received March 25, 2017.

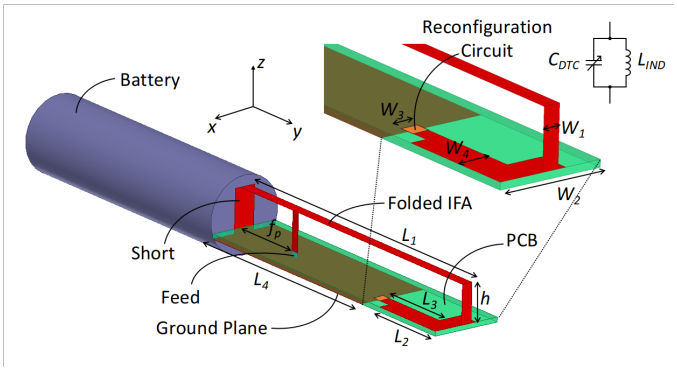

Fig. 1. Structure of the antenna as integrated in the IoT device.

TABLE I
ANTENNA OPTIMIZED GEOMETRICAL PARAMETERS (IN MM).

L_1	L_2	L_3	L_4	f_p	W_1	W_2	W_3	W_4	h
60	18	14	40	15	2	13	1.5	4	7

folded and thus directly printed on the PCB (on the opposite side with respect to the ground plane).

The reason of the folding of the last part of the antenna is twofold. On the one hand, it allows the reduction of the antenna overall volume. On the other hand, and most importantly, it allows an active component to be easily placed in a shunt configuration between the end of the radiator and the ground plane. To enable the connectivity of the electrical component, the width of the very last section of the antenna arm W_3 is allowed to be different from W_4, and the lengths of the antenna and the ground plane are bound to the condition $L_4 + L_3 = L_1$.

The antenna is modeled and designed as integrated in the miniaturized IoT tracking device. A standard AA lithium battery used to power the device (in violet) is electrically connected to the ground plane, thus extending its dimension. The region of the PCB backed by the ground plane ($L_4 \times W_2$) is used to integrate an LPWAN LoRa transceiver operating at 868 MHz, a micro-controller and all the required electronic circuits.

Concerning the design constraints, the whole device must be fit into a cylindrical plastic casing with an outer diameter of 19 mm and a length of 116 mm, corresponding to 0.04λ and 0.35λ at 868 MHz, respectively. Given the presence of the battery, the portion of the cylinder available for the antenna is only 0.17λ long. Moreover, the antenna is required to exhibit a good impedance matching ($|S11| \leq -6$ dB) at the working frequency of 868 MHz. The antenna has been optimized in its passive configuration, i.e., not including any active components. The optimized values of the antenna geometrical descriptors shown in Fig. 1 are summarized in Tab. I. The optimization has been carried out by using a simple trial-and-error procedure, but taking into account that in an IFA structure, the length of the IFA arm is mainly responsible for the resonance position, while the distance between the feed and the short circuit mainly drives the impedance matching.

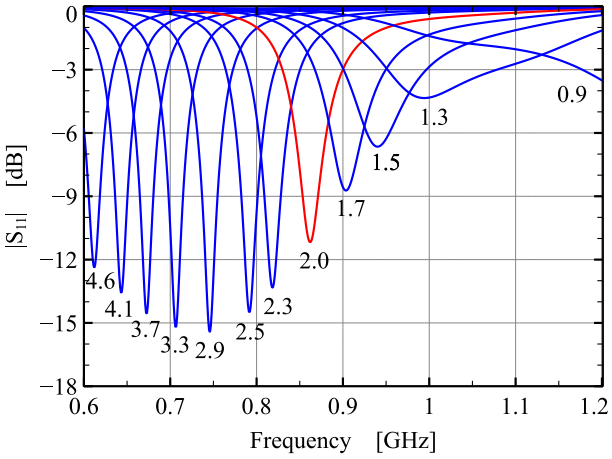

Fig. 2. Antenna resonant frequency for 12 different DTC states.

III. RECONFIGURATION MECHANISM

To enable the frequency tuning of the antenna resonance to compensate the effects of the close environment variations, the proposed solution is to integrate an active reconfigurable component into the radiating structure. Towards this end, a DTC is integrated between the extremity of the IFA arm and the ground plane. This is equivalent to put a variable capacitor in parallel to the RLC model of the antenna, which can be used to modify the resonant frequency of the resulting circuit.

The selected DTC is the PE64906 from Peregrine [12], which provides a shunt capacitance range from 0.9 pF to 4.6 pF with an average serie resistance of 2 Ω. With a 500 μW power consumption, the energy needed by this component is less than 2% compared to the transceiver's one (Semtech SX1275 LoRa module).

The tuning capability comes at the price of a capacitive loading effect that down-shifts the antenna resonance compared to the passive solution. In order to compensate for such an effect and to restore the antenna operation to the desired frequency band, a static inductor is connected in parallel to the DTC. The choice of the inductance value L_{IND} has been made so that it will cancel the DTC capacitance C_{DTC} at 868 MHz. This corresponds to require that the LC circuit composed by the DTC and the inductor would act as open circuit. Consequently, the total impedance of the LC circuit

$$Z_{LC} = \frac{jL_{IND}\omega}{1 - L_{IND}C_{DTC}\omega^2} \tag{1}$$

must tend to infinity (ω being the angular frequency at 868 MHz). Starting from (1), the values of the required inductance L_{IND} and the DTC capacitance C_{DTC} must be selected to verify

$$L_{IND} = \frac{1}{C_{DTC}\omega^2}. \tag{2}$$

Considering the losses of the components, the variation range of the DTC, and in order to verify (2), the following inductance and capacitance values have been selected: $L_{IND} = 15$ nH and $C_{DTC} = 2$ pF.

Fig. 2 shows the effect of selecting 12 different states over the 32 of the DTC on the antenna resonance frequency. The

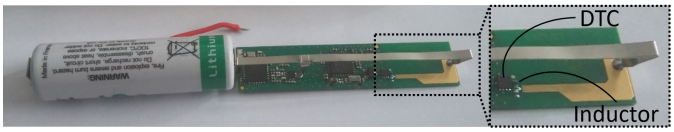

Fig. 3. IoT device prototype including the reconfigurable antenna and zoom on the DTC and the compensating inductor.

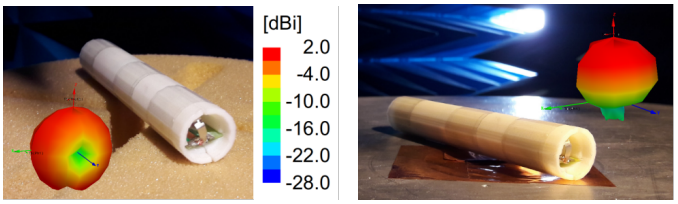

(a) (b)

Fig. 4. Prototype of the device during the measurement phase with sketch of the measured 3d radiation pattern. (a) FS and (b) MS case.

capacitance value provided by each DTC state is reported below the curve. As expected, as the DTC capacitance value increases, the antenna resonant frequency decreases. The state for which the antenna is matched to 868 MHz in free space ($C_{DTC} = 2$ pF) is highlighted in red. As it can be noticed, by considering the $|S11| \leq -6$ dB criteria, the DTC allows the reconfiguration of the antenna resonance over a 46% bandwidth (600 − 960 MHz).

IV. Numerical and Experimental Validation

In order to validate the capability of the antenna to dynamically adapt to the surrounding environment, two extreme scenarios have been considered: (a) when the antenna is in free space (FS) and (b) when the antenna is placed at 5 mm from a 250 × 250 mm^2 metallic surface (MS). In this latter configuration, the 5 mm distance accounts for the presence of the cylindrical plastic casing in which the device is accommodated.

Simulated data are obtained using Ansoft HFSS electromagnetic solver. As for the measurements, a prototype of the antenna is fabricated and assembled with all the electronic components and the battery needed by the IoT device (Fig. 3). All the printed metallic parts are made of copper, while the IFA arm is made of aluminum. To perform radiation pattern measurements, the LoRa transceiver is set to operate in continuous wave (CW) mode with an output power of 14 dBm. The value and stability of the transceiver output power has been assessed connecting the board to a power meter. The Total Radiated Power (TRP) over the entire 3D sphere is measured in a Starlab MVG station. Fig. 4 shows the antenna integrated in the device during the measurement phase in both the FS and MS configurations. The sketches of the measured TRP pattern are also reported to give a qualitative insight of the antenna radiation behavior.

It must pointed out that, the constraints imposed by the application on the antenna geometry basically force the antenna currents to flow lengthwise, thus realizing a short electrical dipole. The radiation pattern in free space has the donut shape

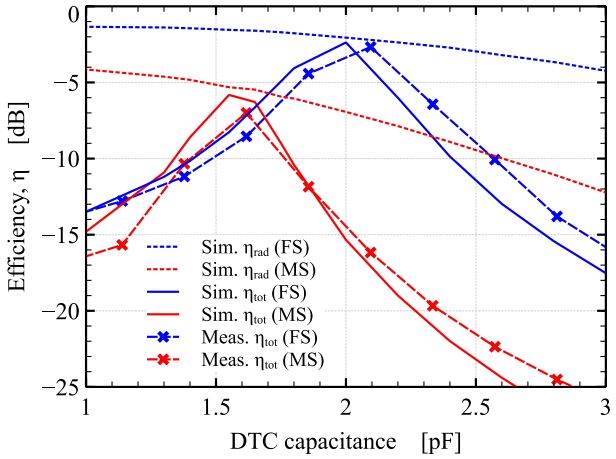

Fig. 5. Simulated and measured efficiency of the reconfigurable antenna at 868 MHz in both the FS and MS scenarios for different DTC capacitance values.

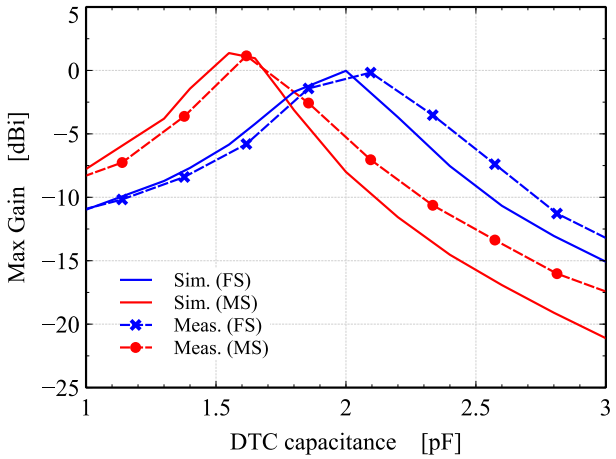

Fig. 6. Simulated and measured total realized peak gain of the reconfigurable antenna at 868 MHz in both the FS and MS scenarios for different DTC capacitance values.

of a classical dipole, as shown in Fig. 4(a). Consequently, the configuration shown in Fig. 4(b) is the worst in terms of modifications to the antenna radiation characteristics caused by the proximity of the metal since the maximum of radiation is in the direction of the metal. Any other position of the device with respect to the metallic plate would result in a minor effect on the antenna radiation characteristics.

Starting from these measurements and exactly knowing the power injected to the antenna, the realized total gain pattern and the total efficiency of the antenna can be extracted. This technical solution has the advantage to avoid the use of a cable to feed the antenna, which would lead to inaccurate measurements given the small antenna dimensions compared to the operating wavelength.

Fig. 5 shows the efficiency of the antenna at 868 MHz for different values of the DTC capacitance. During the measurements, the DTC value is electronically varied by the microcontroller. As it can be observed, a simulated total efficiency of about −2 dB is obtained in free space for 2 pF capacitance value (solid blue line). This is a reasonable

TABLE II
COMPARISON TO THE STATE-OF-THE-ART.

Ref.	Techn.	N. Comp.	N. States	Contr. Volt.	Var. [MHz]
[8]	Varactor	1	Continous	up to 23V	450-900
[9]	Varactor	1	Continous	up to 20V	470-900
[10]	PIN Diodes	4	4	<3V	800-2250
[11]	PIN Diodes	2	4	<3V	700-3550
this	DTC	1	32	<3V	600-950

value considering the compact dimension of the antenna, its folded geometry, and the presence of the DTC component. When the device is placed on a metallic surface (solid red line), the antenna efficiency drops to about -15 dB, making the system inefficient to transmit or receive. The connectivity can be restored by lowering the DTC value to approximately 1.6 pF. This allows the antenna total efficiency to increase to -6 dB, which is acceptable to enable the communication between the device and the base station. A much higher value (-1.78 dB) could be obtained by electrically connecting the metallic surface to the antenna ground plane, however, this would imply specific modifications to the casing and an electrical connection exposed to corrosion. It is worth noting that the decrease of the antenna total efficiency from the FS to the MS case (from -2 to -6 dB) is mainly caused by a 3 dB reduction (from -2 to -5 dB) of the antenna radiation efficiency (dotted lines), as expected for a dipole-like antenna close to a conductor [13]. This demonstrates that a good impedance matching has been restored at the operating frequency of 868. The simulated results are well confirmed by the total efficiency measurements reported in dashed lines.

The realized peak gain of the antenna at 868 MHz is shown in Fig. 6. Following the results obtained in terms of efficiency, the two optimal DTC capacitance values of 2 and 1.6 pF allow the antenna to exhibit approximately 1 and 0 dBi maximum gain in the FS and MS cases, respectively. Despite the lower antenna total efficiency (Fig. 5), the gain increment in the MS scenario compared to the FS case is due to the higher directivity caused by the presence of the metallic surface. This is clearly shown in Fig. 7, where the radiation patterns of the antenna in the two vertical planes at $\varphi = 0^o$ (Fig. 7(a)) and $\varphi = 90^o$ (Fig. 7(b)) are reported. When the device is placed over a metallic surface, the antenna mainly radiates towards the positive z-direction with a patch-like behavior. When the device is in free space, the antenna acts more like an horizontal dipole, with minimum radiation along the device main axis. It must be pointed out that these radiation behaviors are mainly caused by the geometry of the antenna (in FS) and by the presence of the metal plate (in MS). The capacitance introduced by the DTC has a minimum effect on the pattern shapes. Again, measurement data well agree with the numerical simulations. The slight differences in the MS case can be ascribed to the imperfections in realizing the measurement setup with the metal plate with respect to the numerical model.

V. CONCLUSION

This paper has presented a frequency tunable IFA enabling the compensation of the resonance shift produced by the variation of the antenna close surroundings and consequently the maximization of the antenna total efficiency whatever the operating condition. The reconfiguration mechanism is based on the use of a single DTC component, which allows the reconfiguration over 32 different states, and whose very low energy requirement well fits the the long time operation constraints of battery powered IoT devices. These characteristics are summarized in Tab. II and compared to state-of-the-art solutions based on different technologies.

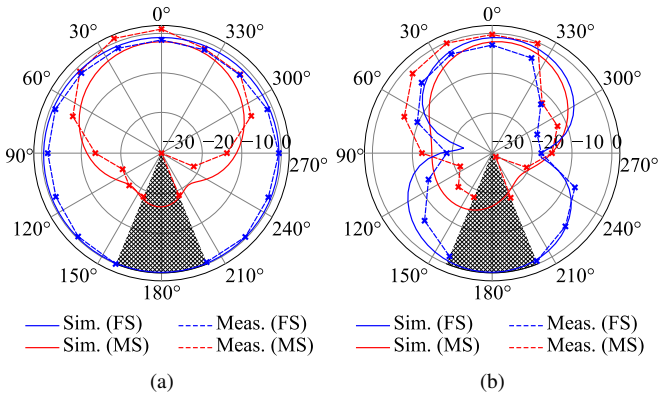

Fig. 7. Measured total realized gain of the reconfigurable antenna at 868 MHz in both the FS and MS scenarios. Vertical planes at (a) $\varphi = 0^o$ and (b) $\varphi = 90^o$. Grey sections indicate the sphere section which cannot be measured by the Starlab station.

In a classical IoT communication scenario, to find the best DCT state, the IoT device could simply sequentially test each state during the transmission phase until the reception of the acknowledgement from the gateway.

The prototype measurements have demonstrated the effectiveness of the proposed solution, which exhibits acceptable efficiency values when the device operates in two very different environment conditions (in free space and over a metallic surface). In comparison to a passive antenna, the total efficiency over a metallic surface can be increased by more than 9 dB. Moreover, the antenna is matched to 50 Ω in the two configurations with a reflection coefficient lower than -10 dB, which guarantees a good linearity of the transceiver power amplifier and an optimal system power consumption.

ACKNOWLEDGMENT

The authors would like to thank the CREMANT for its support.

REFERENCES

[1] J. Petajajarvi, K. Mikhaylov, A. Roivainen, T. Hanninen, and M. Pettissalo, "On the coverage of LPWANs: range evaluation and channel attenuation model for LoRa technology," *14th Int. Conf. ITS Telecomm. (ITST)*, 2015, pp.55-59.

[2] L. Lizzi and F. Ferrero, "Use of ultra-narrow band miniature antennas for internet-of-things applications," *Electron. Lett.*, vol. 51, no. 24, pp. 1964-1966, 2015.

[3] L. Lizzi, F. Ferrero, C. Danchesi and S. Boudaud, "Design of antennas enabling miniature and energy efficient wireless IoT devices for smart cities," *2016 IEEE Int. Smart Cities Conf. (ISC2)*, Trento, Italy, 2016, pp. 1-5.

[4] J. Costantine, Y. Tawk, S. E. Barbin, and C. G. Christodoulou, "Reconfigurable antennas: design and applications," *Proc. of the IEEE*, vol. 103, no. 3, pp. 424-437, 2015.

[5] M. Ng Mou Kehn, Ó. Quevedo-Teruel, and E. Rajo-Iglesias, "Reconfigurable Loaded Planar Inverted-F Antenna Using Varactor Diodes," *IEEE Antennas Wireless Propag. Letters*, vol. 10, pp. 466-468, 2011.
[6] Laure Huitema, Tibault Reveyrand, Jean-Luc Mattei, Eric Arnaud, Cyril Decroze, and Thierry Monediere: "Frequency Tunable Antenna Using a Magneto-Dielectric Material for DVB-H Application", IEEE Transactions on Antennas and Propagation, vol. 61, No. 9, pp. 4456-4466, Sept. 2013.
[7] H. T. P. Thao, V. T. Luan, and V. V.Yem, "Design of compact frequency reconfigurable planar inverf-F antenna for green wireless communications," *IET Commun.*, vol. 10, no. 18, pp. 2567-2574, 2016.
[8] F. A. Asadallah, J. Costantine, and Y. Tawk, "A multiband compact reconfigurable PIFA based on nested slots," *IEEE Antennas Wireless Propag. Letters*, vol. 17, no. 2, pp. 331-334, 2018.
[9] M. P. J. Tiggelman, K. Reimann, F. Van Rijs, J. Schmitz, and R. J. E. Hueting, "On the trade-off between quality factor and tuning ratio in tunable high-frequency capacitors," *IEEE Trans. Electron. Devices*, vol. 56, no 9, pp. 2128-2136, 2009.
[10] J. Ilvonen, R. Valkonen, J. Holopainen, and V. Viikari, "Multiband frequency reconfigurable 4G handset antenna with MIMO capability," *Progress Electromag. Res.*, vol. 148, pp. 233-243, 2014.
[11] R. King, C. Harrison, and D. Denton, "Transmission-line missile antennas," *IRE Trans. Antennas Propag.*, vol. 8, no. 1, pp. 88-90, 1960.
[12] Peregrine Semiconductor, "UltraCMOS® Digitally Tunable Capacitor (DTC) 100 - 3000 MHz," PE64906 datasheet, 2017.
[13] C. A. Balanis, *Antenna Theory: Analysis and Design (3rd ed.)*. Hoboken, NJ: John Wiley, 2005.